Contribution from the Arthur Amos Noyes Laboratory (No. 8348), California Institute of Technology, Pasadena, California 91125, and Bandgap Technology Corporation, Broomfield, Colorado 80021

Electronic Spectra and Photophysics of Platinum(II) Complexes with α-Diimine Ligands. Solid-State Effects. 2. Metal–Metal Interaction in Double Salts and Linear Chains

Vincent M. Miskowski*,[1a] and Virginia H. Houlding*,[1b]

Received November 27, 1990

Solid-state luminescence and absorption data are reported for linear-chain compounds of Pt(II) complexes containing α-diimine ligands in combination with CN^- and amine ligands. Both neutral (e.g. $Pt(bpy)(CN)_2$) and double-salt (e.g. $[Pt(bpy)_2][Pt(CN)_4]$) compounds are examined and compared. All of these compounds have $d(Pt_2)$ near 3.3 Å, and all exhibit strong electronic emission with λ_{max} = 560–715 nm and $k_{rad} = 10^5$–10^6 s^{-1}. This emission is attributed to a $d\sigma^*(d_{z^2}(Pt)) \rightarrow \pi^*(\alpha\text{-diimine})$ triplet-parentage excited state. The assignment is based primarily upon the observed vibronic structure, but correlation with $d(Pt_2)$ is also considered. The factors involved in red-shifting this particular type of metal-to-ligand charge-transfer transition relative to the monomer are discussed, as are criteria for distinguishing metal–metal, charge-transfer, and ligand-localized electronic transitions in Pt(II) α-diimine complexes.

Introduction

We recently reported a study[2] of absorption and emission from Pt(II) coordination complexes containing α-diimine ligands in environments where metal–metal interactions could be considered negligible. We found that truly "monomeric" Pt(II) coordination complexes containing 2,2′-bipyridine (bpy) or 1,10-phenanthroline (phen) exhibit just two types of lowest energy (emissive) excited states. If the complex contains weak-field ligands in addition to a diimine ligand (e.g. $Pt(bpy)Cl_2$), the lowest energy excited state is a triplet ligand field state with a very broad red emission. If the complex contains only strong-field ligands (e.g. $Pt(bpy)(en)^{2+}$ or $Pt(bpy)_2^{2+}$), the lowest energy excited state is a slightly perturbed α-diimine intraligand (IL) $^3(\pi-\pi^*)$ state with a highly vibronic structured green emission. Examples of metal-to-ligand charge transfer (MLCT) emission could not be found for this class of compounds, although some upper excited states could be identified as Pt-to-α-diimine MLCT.

Solid-state electronic spectra of Pt(II) complexes are often perturbed from those of the solution species. In our earlier work[2] we identified one class of weak perturbation as involving "excimeric" interaction between the α-diimine ligands of two or more monomers, resulting in a broad red-shifted $^3(\pi-\pi^*)$ emission. Our prototypical example of this case was the compound $[Pt(phen)_2]Cl_2 \cdot 3H_2O$, which has weak dimers (intermonomer spacing of 3.71 Å)[3] in the crystal.

Pt(II) α-diimine complexes often crystallize in linear-chain structures in which Pt–Pt distances are on the order of 3.0–3.5 Å, leading to stronger perturbation. Examples of such materials include both neutral complexes such as $Pt(bpy)X_2$ (X = Cl,[4] CN[5]) and double salts such as[6] $[Pt(bpy)_2][Pt(CN)_4]$. These materials are generally intensely colored, in contrast to the nearly colorless monomers, and their electronic emissions are likewise distinctive. We will examine several such materials in this paper and will endeavor to show how metal–metal interaction affects electronic absorption and emission spectra, most notably the $Pt \rightarrow \pi^*(\alpha\text{-diimine})$ MLCT transitions.

Experimental Section

The compounds $[Pt(bpy)(en)](ClO_4)_2$, $[Pt(phen)(en)](ClO_4)_2$, $[Pt(phen)_2]Cl_2$, and $[Pt(bpy)_2](ClO_4)_2$ were available from our previous study.[2] The compounds $Pt(bpy)(CN)_2$, $Pt(phen)(CN)_2$, and $Pt(Me_2bpy)(CN)_2 \cdot 2H_2O$ (where Me_2bpy is 5,5′-dimethyl-2,2′-bipyridine) were prepared by the methods of ref 5; we thank Dr. C.-M. Che for donating samples of these compounds that were used in our initial studies.

The double-salt compounds with $Pt(CN)_4^{2-}$ anions listed in Table I were prepared by coprecipitation from aqueous solutions according to literature methods.[4b,6] These compounds usually precipitate as yellow hydrates which readily lose water upon washing with organic solvent, vacuum-drying, or, in some cases, simply standing in air, yielding the intensely colored (usually deep orange to red) anhydrous forms. The double salts $[Pt(bpy)_2][Pt(CN)_4]$, $[Pt(phen)_2][Pt(CN)_4]$, and $[Pt(phen)(en)][Pt(CN)_4]$ all formed hydrates. Satisfactory elemental analyses were obtained for the anhydrous forms; the hydrates analyzed well for relative values of C, N, and Pt but were not generally robust enough to yield reproducible values of hydration number.

The previously unreported compound $[Pt(bpy)(en)][Pt(CN)_4]$ was the only double salt that did not initially precipitate as a hydrate. It was prepared by slow addition of a stoichiometric amount of an aqueous solution of $Na_2Pt(CN)_4$ to slow addition of a stoichiometric amount of an aqueous solution of $Na_2Pt(CN)_4$ to a hot (60 °C stirred aqueous solution of $[Pt(bpy)(en)](ClO_4)_2$. After the mixture was cooled to room temperature, the bright yellow precipitate was filtered off and washed with water, ethanol, and ether. Vacuum-drying overnight left the color unchanged, and an elemental analysis indicated an anhydrous formulation for the yellow solid. Anal. Calcd (found) for $Pt_2C_{16}H_{16}N_8$: C, 26.45 (26.18); H, 2.22 (2.37); N, 15.42 (15.43).

Powder X-ray diffraction spectra of two representative double salts, $[Pt(bpy)(en)][Pt(CN)_4]$ and anhydrous $[Pt(bpy)_2][Pt(CN)_4]$, were obtained on a Phillips APD3600 diffractometer using Cu Kα radiation and were indexed by a combination of manual and iterative computer fitting. Transmission electron microscopy (TEM) was used to collect electron diffraction micrographs of single microcrystals (ca. 20 × 500 μm needles) of $[Pt(bpy)(en)][Pt(CN)_4]$ for comparison with the powder X-ray diffraction data. Hydrated salts were not stable to either of these techniques.

Emission, absorption, and lifetime measurements in general employed the equipment and methods of ref 2. For measurements made on hydrated forms, samples were stored and examined as aqueous slurries or colloids. Emission lifetime measurements on hydrated samples were unsuccessful; intense coloration (indicative of dehydration) developed immediately upon exposure of samples to laser pulses. Several nanosecond time scale emission lifetime measurements were performed at The Center for Fast Kinetics, The University of Texas, Austin, TX.

Results

Monomers. In order to facilitate a discussion of the solid-state effects on the electronic structure of strongly interacting materials, it is useful to consider first the structure of the analogous monomeric Pt(II) complexes. We have discussed the electronic absorption and emission spectra of several monomeric Pt(II) α-diimine complexes in considerable detail in ref 2, including $Pt(bpy)_2^{2+}$, $Pt(phen)_2^{2+}$, and $Pt(bpy)(en)^{2+}$. The reader is also referred to refs 7–10 for other recent work concerning the spectra

(1) (a) California Institute of Technology. (b) Bandgap Technology Corp.
(2) Miskowski, V. M.; Houlding, V. H. *Inorg. Chem.* **1989**, *28*, 1529.
(3) Hazell, A.; Mukhopadhyay, A. *Acta Crystallogr.* **1980**, *B36*, 1647.
(4) (a) Textor, M.; Oswald, H. R. *Z. Anorg. Allg. Chem.* **1974**, *407*, 244. (b) Osborn, R. S.; Rogers, D. *J. Chem. Soc., Dalton Trans.* **1974**, 1002. (c) Bielli, E.; Gidney, P. M.; Gillard, R. D.; Heaton, B. T. *J. Chem. Soc., Dalton Trans.* **1974**, 2133.
(5) Che, C.-M.; He, L.-Y.; Poon, C. K.; Mak, T. C. W. *Inorg. Chem.* **1989**, *28*, 3081.
(6) (a) Little, W. A.; Lorentz, R. *Inorg. Chim. Acta* **1976**, *18*, 273. (b) Kiernan, P. M.; Ludi, A. *J. Chem. Soc., Dalton Trans.* **1978**, 1127. (c) Houlding, V. H.; Frank, A. J. *Inorg. Chem.* **1985**, *24*, 3664.
(7) Maestri, M.; Sandrini, D.; Balzani, V.; von Zelewsky, A.; Deuschel-Cornioley, C.; Jolliet, P. *Helv. Chim. Acta* **1988**, *71*, 103.

0020-1669/91/1330-4446$02.50/0

Table I. Photophysical Properties of Linear-Chain Pt(II) Compounds[a]

compd (powder color)	λ_{max}, nm: diffuse reflectance	λ_{max}, nm: emission excitation	λ_{max}, nm: emission	emission lifetime τ, ns	emission quantum yield[b]	calcd k_r, s^{-1}
[Pt(bpy)(en)][Pt(CN)$_4$] (bright yellow)	330, 450	500 (sh)	560 (584, 30 K)	160	0.17 (0.30, 30 K)	1.1×10^6
[Pt(phen)(en)][Pt(CN)$_4$] (bright yellow)	310, 430	500 (sh)	560	150	intense[c]	
[Pt(bpy)$_2$][Pt(CN)$_4$]·2H$_2$O[d] (yellow)	485	500 (sh)	570	<15	weak[c]	
[Pt(bpy)$_2$][Pt(CN)$_4$] (orange)	330, 520	530 (sh) (548, 20 K)	620 (658, 20 K)	8 (690, 77 K)	0.002	2.5×10^5
[Pt(phen)$_2$][Pt(CN)$_4$] (violet)	310, 380, 550	c	650	<15	weak[c]	
Pt(bpy)(CN)$_2$·xH$_2$O (yellow)	c	c	571	c	c	
Pt(bpy)(CN)$_2$ (orange)	340, 490	549 (544, 30 K)	600 (655, 30 K)	160	0.041 (0.091, 30 K)	2.6×10^5
Pt(phen)(CN)$_2$ (red)	310, 375, 520	580 (572, 30 K)	715 (775, 30 K)	130	0.030 (0.11, 30 K)	1.8×10^5

[a] Entries are for room temperature except as indicated (values in parentheses). Emission parameters are corrected for instrumental factors. [b] Measured by the powder method of: Wrighton, M. S.; Ginley, D. S.; Morse, D. L. *J. Phys. Chem.* **1974**, *78*, 2229. [c] Not measured. [d] See also ref 6c for colloid data.

of monomeric Pt(II) α-diimines, particularly Pt(α-diimine)(CN)$_2$ complexes.[9-11] There are several generalizations that apply to these complexes.

First, all of the complexes to be discussed have strong ligand fields, and all ligand field (LF) absorption features, both singlet and triplet, are predicted[2] by analogy to Pt(II) tetraamine complexes to be below 350 nm. Not only are they completely hidden by intense diimine $^1(\pi-\pi^*)$ (^{1}IL) and Pt-to-diimine charge-transfer (^{1}MLCT) absorption bands, but they are also too high in energy to be considered as candidates for the emissive state. Similarly, MLCT absorption involving CN^- is found at wavelengths below 270 nm;[12] there is no reason to invoke participation of CN^- or en in any of the low-lying excited states.

The second important point is that the energies of diimine ^{1}IL and ^{1}MLCT absorption features are not significantly affected by the nature of the other ligands for these ligand sets. The spectra of Pt(II) complexes containing bpy show intense structured absorption in the region 300–320 nm, which is assigned as ^{1}IL. Phen complexes show analogous absorption in the region 350–390 nm. The less intense ^{1}MLCT absorption occurs in the same region as diimine intraligand absorption and is often partially or wholly obscured. For example, in the absorption spectrum of Pt(bpy)(en)$^{2+}$ in acetonitrile, the MLCT band appears as a shoulder at ~330 nm, and the absorption spectrum of Pt(Me$_2$bpy)(CN)$_2$ is very similar.[9,11]

The third point is that the singlet–triplet splitting of the IL state is apparently larger than that of the diimine MLCT state. Spin-forbidden IL and MLCT absorptions both lie in the region 400–500 nm, which complicates direct assignment of the observed features. However, in all of the strong-field monomeric Pt^{II}(α-diimine)$_2$ and Pt^{II}(α-diimine)(acidoamine)$_2$ complexes considered here, a ^{3}IL state is the lowest excited state,[2,9,10] giving rise to a distinctive highly structured green emission both in dilute solution (room temperature or low-temperature glass), and in crystalline matrices where the complexes may be considered noninteracting.

Linear-Chain Solids: Double Salts. Linear-chain Pt(II) materials, including ions such as Pt(CN)$_4^{2-}$, and double salts such as Magnus' green salt[13] ([Pt(NH$_3$)$_4$][PtCl$_4$]), have been known for many years, and have been the subject of extensive study.[14] The structures of these materials generally feature linear chain stacks of square-planar complexes (alternating anions and cations in the case of double salts), with Pt–Pt distances of the order of 3.0–3.5 Å. The electronic spectra[15] of Pt(II) double salts are strongly perturbed from those of the monomeric constituents, which is attributable to Pt–Pt interactions. In addition to being strongly colored, these materials are often luminescent at room temperature,[12] again in contrast to the behavior of discrete monomers.[2,16]

The Pt(II) α-diimine double-salt compounds to be considered here all involve the anion Pt(CN)$_4^{2-}$. As far as we are aware, the crystal structure of a double salt involving the Pt(CN)$_4^{2-}$ anion has not yet been reported, presumably because these salts are often very insoluble and thus difficult to crystallize. However, [Pt(bpy)(en)][Pt(CN)$_4$] was found to be highly crystalline according to optical microscopy, powder X-ray diffraction (66 reflections observed), and TEM electron diffraction.

The X-ray data for [Pt(bpy)(en)][Pt(CN)$_4$] were best indexed by an orthorhombic unit cell: a = 12.54 Å, b = 11.16 Å, c = 6.68 Å, unit cell volume 934.8 Å^3.[17] This unit cell volume is extremely reasonable. The reported structures of Pt(bpy)(CN)$_2$,[5] "red" Pt(bpy)Cl$_2$,[4a,b] and Pt(en)Cl$_2$,[18] all of which crystallize in stacked

(8) (a) Ballardini, R.; Gandolfi, M. T.; Balzani, V.; Kohnke, F. H.; Stoddart, J. F. *Angew. Chem., Int. Ed. Engl.* **1988**, *27*, 692. (b) Ballardini, R.; Gandolfi, M. T.; Prodi, L.; Ciano, M.; Balzani, V.; Shahriar-Zavarah, H.; Spencer, N.; Stoddart, J. F. *J. Am. Chem. Soc.* **1989**, *111*, 7072.

(9) Che, C.-M.; Wan, K.-T.; He, L. Y.; Poon, C.-K.; Yam, V. W.-W. *J. Chem. Soc., Chem. Commun.* **1989**, 943.

(10) Kunkely, H.; Vogler, A. *J. Am. Chem. Soc.* **1990**, *112*, 5625.

(11) We note that the electronic spectra are insensitive to alkylation of the α-diimine ligand. For example, the electronic absorption, emission, and excitation spectra of Pt(Me$_2$bpy)Cl$_2$ in butyronitrile solution are nearly indistinguishable from those of[2] Pt(bpy)Cl$_2$ under the same conditions.

(12) Gliemann, G.; Yersin, H. *Struct. Bonding* **1985**, *62*, 87. The absorption spectrum of the compound Pt(en)(CN)$_2$ has also been reported: Isci, H.; Mason, W. R. *Inorg. Chem.* **1975**, *14*, 905. It is similar to that of Pt(CN)$_4^{2-}$ but slightly blue-shifted.

(13) Magnus, G. *Pogg. Ann.* **1828**, *14*, 242. For the crystal structure, see: Atoji, M.; Richardson, J. W.; Rundle, R. E. *J. Am. Chem. Soc.* **1957**, *79*, 3017.

(14) See work cited in: (a) Thomas, T. W.; Underhill, A. E. *Chem. Soc. Rev.* **1972**, *1*, 99. (b) Interrante, L., Ed. *Extended Interactions Between Metal Atoms*; American Chemical Society: Washington, DC, 1974. (c) Keller, H. J., Ed. *Low Dimensional Cooperative Phenomena*; Plenum Press: New York, 1975. (d) Keller, H. J., Ed. *Chemistry and Physics of One-Dimensional Metals*; Plenum Press: New York, 1977. (e) Miller, J. S., Ed. *Extended Linear Chain Compounds*, Plenum Press: New York, 1982.

(15) (a) Martin, D. S., Jr. In ref 14e, pp 409–451. (b) Anex, B. G.; Ross, M. E.; Hedgecock, M. W. *J. Chem. Phys.* **1967**, *46*, 1090.

(16) To our knowledge, emission from Pt(CN)$_4^{2-}$ *monomers* has never been established, although emission from oligomers in solution is known: (a) Lechner, A.; Gliemann, G. *J. Am. Chem. Soc.* **1989**, *111*, 7469. (b) Schindler, J. W.; Fukuda, R. C.; Adamson, A. W. *J. Am. Chem. Soc.* **1982**, *104*, 3596.

(17) We have not attempted intensity refinement of these data, since the molecular unit is far more complex than usual for intensity refinements of powder X-ray data. Attempts to index a monoclinic cell gave a fit to a refined value of β of 92.7°, which is not distinguishable from 90° by our powder X-ray data. The orthorhombic cell is preferred because, for several TEM micrographs, the ratio method of indexing the reflection patterns of single microcrystals (Thomas, G. *Transmission Electron Microscopy of Metals*; Wiley-Interscience: New York, 1962) yielded a good fit only when β was set at 90°.

structures with Pt–Pt distances in the range 3.33–3.45 Å, yield "molecular volumes" for these compounds of respectively 283, 273, and 170 Å^3. Assuming a similar $d(Pt_2)$, we can use these values to estimate a molecular volume for $[Pt(bpy)(en)][Pt(CN)_4]$ as $(2 \times 283) - 273 + 170 = 466$ Å^3. Thus, the powder X-ray indexing is consistent with $Z = 2$. The only reasonable candidate among the orthorhombic axes for a metal-stacking axis is the c axis. This would give a $d(Pt_2)$ of 3.34 Å, since the repeat distance should be (at a minimum) twice the $d(Pt_2)$. Observed reflection intensities are consistent with this hypothesis. In particular, the two most intense reflections are indexed (110) and (002), a result also obtained in the diffraction pattern of the orthorhombic linear-chain "red" $Pt(bpy)Cl_2$.[4a]

Electron diffraction patterns of single microcrystals of $[Pt(bpy)(en)][Pt(CN)_4]$, obtained by TEM, are consistent with this orthorhombic cell except that they show weak reflections for favorably oriented crystals that correspond to a doubled c axis. Thus, the true unit cell is likely to be c-centered (or some related crystallographic condition exists that would yield weak or missing (001) reflections for odd values of l). In summary, these data provide strong support for the hypothesis of a metal-stacking axis along the c axis.

Powder X-ray data on the anhydrate of the double salt $[Pt(bpy)_2][Pt(CN)_4]$ indicated moderate crystallinity, 20 broad (fwhm ≥1°) reflections being observed. The method of sample preparation, dehydration of a crystalline solid, is probably responsible for the poor quality of the powder X-ray spectrum; the extreme insolubility of this material in any known solvent has prevented the preparation of more highly crystalline samples. The data were computer-indexed to an orthorhombic unit cell: a = 9.502 Å, b = 8.357 Å, c = 3.623 Å, cell volume 287.7 Å^3. Since the unit cell volume of the linear-stack isomer $Pt(bpy)(CN)_2$ has been found by single-crystal X-ray determination[5] to be 565.6 Å^3 ($Z = 2$), the orthorhombic cell volume is quite reasonable if it is assumed that the true cell volume should be a multiple of the indexed value. There is not, however, a good candidate for a metal-stacking axis among the orthorhombic axes; the c-axis spacing seems far too long for a Pt–Pt distance by comparison to 3.3296 Å for the $Pt(bpy)(CN)_2$ structure.[5] While compounds of this type usually exhibit chains parallel to a crystallographic axis, there is, of course, no requirement that they do so. It is possible that a simpler description of the structure might arise in monoclinic symmetry, but the low quality of the data prevented any meaningful attempts at monoclinic fits. The agreement of the unit cell volume found for this material with that of $Pt(bpy)(CN)_2$, together with the similar color and solid-state spectral features (vide infra), do suggest a chain structure with a similar $d(Pt_2)$ of ~3.3 Å.

All $[Pt^{II}(\alpha\text{-diimine})][Pt(CN)_4]$ double-salt compounds that we have examined are more strongly colored[4b,6] than the separate constituents and are invariably luminescent,[6c] which suggests Pt–Pt interactions. It is likely that these $Pt(CN)_4^{2-}$ double salts all adopt a linear-chain stacked structure similar to those discussed above, and we will assume so in the following discussion. A summary of spectroscopic data for these materials can be found in Table I. Some of the spectroscopic properties of these materials have been previously reported in ref 6 and are reproduced here for the sake of clarity. The spectra of two salts, $[Pt(bpy)(en)][Pt(CN)_4]$ and $[Pt(bpy)_2][Pt(CN)_4]$, will be examined in detail as representative of this class of materials. Two additional double salts, $[Pt(phen)(en)][Pt(CN)_4]$ and $[Pt(phen)_2][Pt(CN)_4]$, have also been investigated, and results are included in Table I. They are very similar to their bpy analogues.

The emission spectra of crystalline $[Pt(bpy)(en)][Pt(CN)_4]$ at room temperature and 30 K are shown in Figure 1. Photophysical and spectroscopic parameters are listed in Table I. This compound is strongly emissive even at 300 K, the emission profile being highly asymmetric to lower energy. At 30 K, the emission has red-shifted significantly; this is typical behavior for metal–metal-stacked

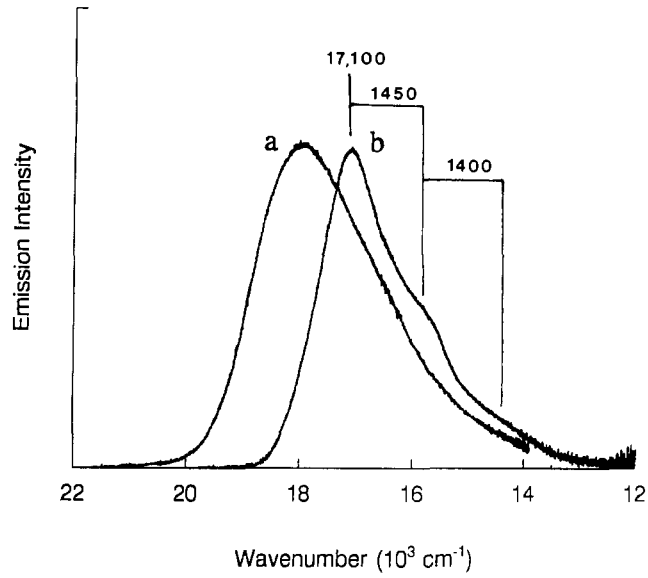

Figure 1. Corrected emission spectra for $[Pt(bpy)(en)][Pt(CN)_4]$ at (a) room temperature and (b) 30 K. The spectra are normalized to equal height; the T = 30 K peak intensity is actually ~2.5 times that at room temperature. Emission maximum and vibronic intervals of the low-temperature spectrum are given in units of cm^{-1}.

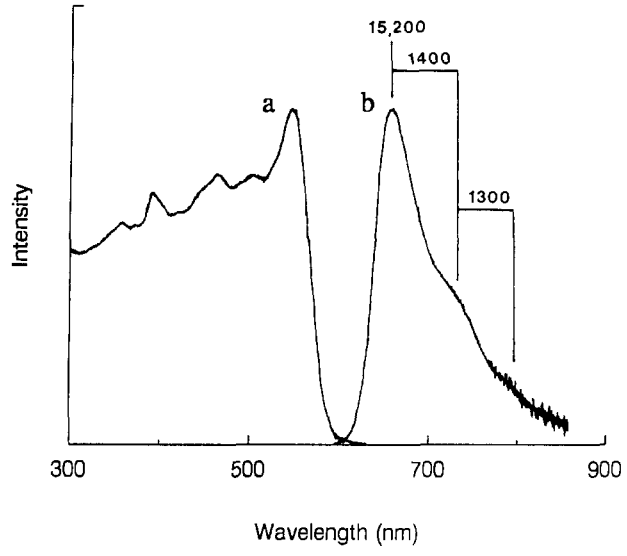

Figure 2. Corrected (a) emission and (b) excitation spectra for $[Pt(bpy)_2][Pt(CN)_4]$ at 20 K. Spectral slit width = 2 nm. Emission maximum and vibronic intervals of the low-temperature spectrum are given in units of cm^{-1}.

compounds and is attributable[12] to metal–metal bond shortening as a result of thermal lattice contraction. The emission has also narrowed, and shoulders have developed out of the long-wavelength tail. The energetic spacing of these features is ~1400 cm^{-1}, and the vibronic pattern is characteristic of an excited-state distortion of the bpy ligand.[2,19] The vibronic spacings and relative vibronic intensities are similar to those observed for thoroughly established MLCT states of $Ru(bpy)_3^{2+}$ and related compounds.[19] The ~1400-cm^{-1} vibronic interval can be attributed to an "average" bpy vibrational frequency.[19b] It is noteworthy that the Huang–Rhys constant S, defined by the vibronic intensity ratio $I(1,0)/I(0,0)$, is only ~0.5 compared to the value of ~1.4 observed for the ^{3}IL emission of the isolated $Pt(bpy)(en)^{2+}$ cation,[2] indicating a considerably smaller Franck–Condon factor. This is also very

(18) Iball, J.; MacDougal, M.; Scrimgeour, S. *Acta Crystallogr.* **1975**, *B31*, 1672.

(19) (a) Myrick, M. L.; Blakley, R. L.; DeArmond, M. K.; Arthur, M. L. *J. Am. Chem. Soc.* **1988**, *120*, 1325. (b) Caspar, J. V.; Westmoreland, T. D.; Allen, G. H.; Bradley, P. G.; Meyer, T. G.; Woodruff, W. H. *J. Am. Chem. Soc.* **1984**, *106*, 3492. (c) Hager, G. D.; Crosby, G. A. *J. Am. Chem. Soc.* **1975**, *97*, 7031.

much in keeping with a MLCT assignment for the double-salt emission; bpy excited-state distortions should be roughly twice as large in the IL states as in the MLCT states, since the ligand π-bond orders are decreased by approximately twice as much in the IL states. Thus, the Franck–Condon factor (as indicated by the Huang–Rhys ratio) provides a way of distinguishing between IL and MLCT emission in this particular case.

Emission data for the compound $[Pt(bpy)_2][Pt(CN)_4]$ are shown in Figure 2. The emission is very similar to that of the preceding compound, but red-shifted by 1800 cm^{-1}. The yellow dihydrate, which is the initial precipitate of this compound from aqueous solution, shows room-temperature emission (Table I) that is nearly identical with that of $[Pt(bpy)(en)][Pt(CN)_4]$, although it is considerably less intense. According to the extensive data base that is available for $Pt(CN)_4^{2-}$ salts,[12] blue-shifted emission should correlate to a longer Pt_2 distance. It indeed seems reasonable that either lattice water or the nonplanar en ligand might impose slightly longer Pt_2 separations that would occur in their absence.

Figure 2 also shows a luminescence excitation spectrum for anhydrous $[Pt(bpy)_2][Pt(CN)_4]$; it displays a well-defined band maximizing at 548 nm that bears a mirror-image relationship to the emission. The excitation spectrum at shorter wavelengths is highly distorted.[20] In our experience, an absorption band of a concentrated solid must be quite weak ($\epsilon < 10^2$) for it to appear as a well-defined band in an emission excitation spectrum, and this presumably applies to the 548-nm feature. Each of the other double-salt compounds similarly shows an excitation maximum about 3000 cm^{-1} above the emission maximum (Table I), and this absorption presumably corresponds to the emissive state.

We have recorded diffuse-reflectance spectra of these compounds (Table I). Each shows one or more intense bands below 400 nm that are very similar to those of the dilute monomer spectra (vide supra; also ref 2), and similar ^{1}IL assignments are assumed. There is, in addition, a strong absorption band in the visible region that is responsible for the intense color of each material (see also ref 6c). In each case it is significantly blue-shifted relative to the lowest energy excitation maximum. We postulate that the emission and lowest energy excitation maxima represent a formally spin-forbidden ^{3}MLCT transition and that the intense absorption band seen in the reflectance spectra (and also in colloid absorption spectra[6c]) is the corresponding ^{1}MLCT transition. The ^{1}MLCT band presumably has been red-shifted from its monomer position by axial Pt–Pt interactions in the crystal lattice, which may be compared to the strong solvent effect seen in the case of the ^{1}MLCT band of $Pt(bpy)Cl_2$.[21]

Both quantum yields and lifetimes have been determined for the luminescence of $[Pt(bpy)(en)][Pt(CN)_4]$ and anhydrous $[Pt(bpy)_2][Pt(CN)_4]$, so radiative rate constants (k_r) could be calculated (Table I). Given the observed emission half-widths of 2500–3000 cm^{-1} at room temperature and 1500–2000 cm^{-1} at low temperature for all of the compounds, the observed values of $k_r = 10^5$–10^6 s^{-1} correspond to an ϵ_{max} of 50–500 for the corresponding absorption band, according to a Strickler–Berg calculation,[22] which is consistent with our assignment of the excitation spectrum. We note that several of these compounds showed, in addition to the exponential nanosecond to microsecond emission decay lifetimes that are listed in Table I, subnanosecond "spikes" of fast emission decay. These could conceivably represent a singlet–singlet fluorescence; a weak fluorescence (in addition to intense phosphorescence) has been established[23] for the binuclear

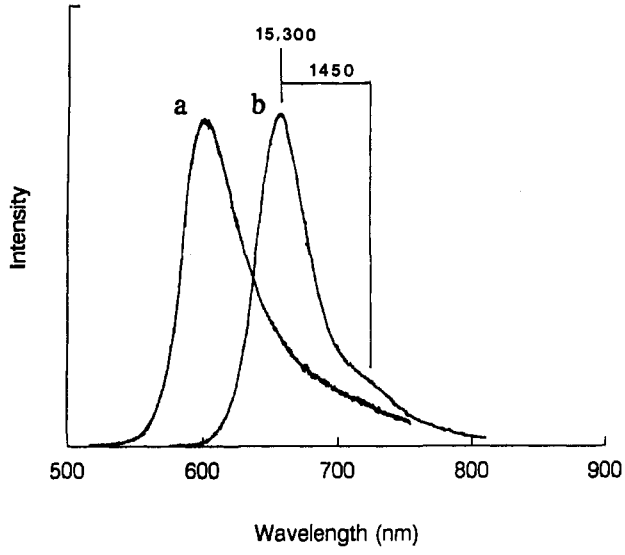

Figure 3. Corrected emission spectra for $Pt(bpy)(CN)_2$ at (a) room temperature and (b) 30 K. The spectra are normalized to equal height; the T = 30 K peak intensity is actually about 3 times that at room temperature. Emission maximum and vibronic intervals of the low-temperature spectrum are given in units of cm^{-1}.

Pt(II) complex $Pt(P_2O_5H_2)_4^{4-}$. However, it is difficult to exclude artifacts in solid-state powder experiments of the type we have performed, and we are therefore not confident about these signals. In any case, the short-lived signal does not make an observable contribution to the static emission spectrum at either room temperature or low temperature in any of the compounds.

Linear-Chain Solids: Neutral Stacks. We include data for three "neutral-stack" Pt(α-diimine)$(CN)_2$ compounds in Table I. Note that each of them is formally an isomer of one of the double salts discussed in the preceding section. They are distinguished from the double-salt isomers by being slightly soluble[4b,5] in polar solvents such as dimethylformamide and dimethyl sulfoxide. Similar to the double-salt materials, yellow hydrates are obtained as the initial products from aqueous solution; the ansolvous solids are highly colored (red or purple), which again suggests the presence of Pt–Pt interactions.[4b] Che et al.[5] have reported the crystal structure of $Pt(bpy)(CN)_2$. It features strictly linear infinite chains, with a Pt_2 spacing of 3.3296 Å.

The data in Table I show that the neutral-stack and double-salt isomers have remarkably similar spectroscopic and photophysical properties; the only difference of note is that the room-temperature emission lifetimes of the neutral-stack compounds tend to be longer, the quantum yields being proportionately higher. This indicates that k_r is roughly the same for the emissive states of the neutral-stack and double-salt isomers, thus suggesting a basic electronic similarity. Faster nonradiative decay processes (k_{nr}) apparently occur for the double salts at room temperature. This difference is of doubtful significance to fundamental electronic structure. The neutral-stack compounds are undoubtedly of higher crystallinity than the double-salt samples, since they were soluble enough to be recrystallized. They are likely to have longer average chain lengths and hence lower densities of "dark traps"[24] (nonemissive excitation quenchers) caused by vacancies, dislocations, or stacking faults.

(20) That is, it is "topped off" because the solid is so strongly absorbing that essentially all of the excitation light is absorbed in a thin surface layer. Various nonlinear effects such as excited-state absorption and stimulated scattering can also contribute to deviations from the optically dilute absorption spectrum.

(21) Gidney, P. M.; Gillard, R. D.; Heaton, B. T. *J. Chem. Soc., Dalton Trans.* **1973**, 132.

(22) Porter, G. B. In *Concepts of Inorganic Photochemistry*; Adamson, A. W., Fleischauer, P. D., Eds.; Wiley-Interscience: New York, 1975; Chapter 2.

(23) Stiegman, A. E.; Rice, S. F.; Gray, H. B.; Miskowski, V. M. *Inorg. Chem.* **1987**, *26*, 1112.

(24) It has been shown that intentional introduction of dark traps (for example, $Ni(CN)_4^{2-}$)[25] into linear-chain $Pt(CN)_4^{2-}$ salts results in pronounced emission quenching, particularly at room temperature. We have prepared analogous Ni-doped samples of $[Pt(bpy)_2][Pt(CN)_4]$ with up to 10% replacement of $Pt(CN)_4^{2-}$ by $Ni(CN)_4^{2-}$ and have observed very strong quenching, indicative[26] of excited-state mobility on the order of 50–100 repeat units. Thus, a small increase in dark traps such as chain ends is expected to give rise to significant emission quenching.

(25) Schultheiss, R.; Hidvegi, I.; Gliemann, G. *J. Chem. Phys.* **1983**, *79*, 4167.

(26) (a) Onipko, A. I.; Malysheva, L. I.; Zozlenko, I. V. *Chem. Phys.* **1988**, *121*, 99. (b) Blanzat, B.; Barthou, C.; Tercier, N.; Andre, J.-J.; Simon, J. *J. Am. Chem. Soc.* **1987**, *109*, 6193.

This is a fundamental problem of solid materials, but an interesting one, since it relates to excitation mobility, which is of importance for photochemical and photovoltaic applications.[6b] In this connection we add that the puzzling disagreement of our measured value of 160 ns for the room-temperature-emission lifetime of $Pt(bpy)(CN)_2$ (Table I) with those of ref 5 (240 ns) and ref 27a (~ 2 μs) may possibly reflect differences in sample preparation and history for the materials upon which measurements were performed by the various groups. Readers familiar with semiconductor or organic polymer photophysical properties will not be surprised by this caveat. Much additional research will be required to address this point in an adequate fashion. However, we note that the shapes of emission spectra of these materials are very reproducible, our data also comparing well to those of other groups,[5,27a] so it is reasonable to assume that the emissions are "intrinsic" and that our observations do pertain to the linear-chain chromophores, although the rates of nonradiative decay may have a more complicated genesis.

Figure 3 shows the emission spectra of $Pt(bpy)(CN)_2$ at room temperature and 30 K, which indicate one additional difference from the double-salt isomer $[Pt(bpy)_2][Pt(CN)_4]$. While vibronic structure in an effective frequency of ~ 1400 cm^{-1} is observed, the Franck–Condon factor is smaller. The Huang–Rhys ratio S for the double salt is ~ 0.5, while that for $Pt(bpy)(CN)_2$ is ~ 0.25. Very similar emission spectra and vibronic patterns were observed for the other neutral-stack compounds of Table I, with emission maxima that vary with α-diimine ligand very similarly to those of the isomeric double salts.

The single-crystal absorption and emission spectra of $Pt(\alpha\text{-diimine})(CN)_2$ materials have been studied extensively by Gliemann and co-workers,[27] and we will discuss their results[27a,28] for $Pt(bpy)(CN)_2$ as a representative example. At 1.9 K, intense phosphorescence (τ = 2ms) is observed polarized perpendicular to the Pt-stacking axis. The maximum (654 nm) and spectral profile of this emission are essentially identical with our own data for powder samples at 30 K, although our spectrum extends to longer wavelength and clearly shows the vibronic (~ 1400 cm^{-1}) sidebands. A higher energy fluorescence (λ_{max} = 620 nm, $\tau <$ 3 ns) with similar band shape is also reported, having polarization parallel to the Pt-stacking axis. We did not see a resolved fluorescence in our powder experiments; self-absorption of the fluorescence via singlet–triplet absorption by the powder presumably accounts for this.

Polarized single-crystal absorption spectra at 10 K were also reported. The absorption with light polarized parallel to the Pt–Pt stacking direction was far too intense to be recorded for the single crystals; the strong visible absorption (see Table I) that is responsible for the material's orange-red color is evidently polarized parallel to Pt–Pt. For light polarized perpendicular to the stacking axis, however, a relatively weak (ϵ = 150[29]), sharp absorption band was observed at 18 450 cm^{-1} (542 nm) and assigned to the emissive triplet state. This band is essentially coincident with our lowest energy excitation maximum. An unassigned shoulder (labeled II in ref 27a) at 19 850 cm^{-1} (ϵ = 30[29]), 1400 cm^{-1} above the first absorption, corresponds extremely well in both spacing and relative intensity to the vibronic sideband we have observed in the emission spectrum. Thus, a mirror-image relationship appears to exist between absorption and emission for the phosphorescence.

Three additional very weak absorption features (labeled III–V)[27a] were reported at 22 300, 23 750, and 25 400 cm^{-1}, respectively. It is noteworthy that these features agree extremely well with features reported by us[2] for *monomeric* Pt(II) α-diimine complexes such as $Pt(bpy)(en)^{2+}$, which we assigned to the lowest energy ^{3}IL transition, the emissive state of the isolated chromophores. (The spacings of lines III–V are attributable to bpy vibrational modes.) It therefore appears that the α-diimine ^{3}IL transition is note greatly perturbed by the metal-stacked structure, which is consistent with our reflectance data (Table I) for the ^{1}IL transitions.

Discussion

We shall first review the classes of electronic spectral behavior that can result from metal–metal interaction of square-planar d^8 metal ion complexes such as those of Pt(II).

Binuclear metal complexes are typified[22,30] by the complex $Pt_2(P_2O_5H_2)_4^{4-}$, which has a Pt_2 bond distance of 2.922 Å. This complex exhibits both fluorescence (weak, $\tau \simeq 8$ ps) at 399 nm and phosphorescence (intense, τ = 9.8 μs) at 513 nm. The former is polarized parallel to the Pt_2 (molecular z) axis, while the latter is polarized perpendicular to the Pt_2 axis (that is, molecular x,y-polarization). These emissions have been assigned to transitions from the $^1A_{2u}$ ($d\sigma^*$–$p\sigma$) and $E_u(^3A_{2u})$ ($d\sigma^*$–$p\sigma$) excited states, respectively; the $^3A_{2u}$ state gives rise to spin–orbit components of E_u and A_{1u} symmetry,[30,31] with transitions between the A_{1u} component and the $^1A_{1g}$ ground state being dipole-forbidden in D_{4h} symmetry. Corresponding absorption features are found[23] at 367 nm (ϵ = 34 500, $^1A_{2u}$, z-polarized) and 452 nm (ϵ = 110, $E_u(^3A_{2u})$, x,y-polarized). These transitions have been explained in terms of a simple MO model in which the Pt(II) filled d_{z^2} and empty p_z orbitals both interact in the dimer to split into bonding (stabilized) and antibonding (destabilized) combinations, with the result that $d\sigma^* \rightarrow p\sigma$ transitions are strongly stabilized relative to monomer $d_{z^2} \rightarrow p_z$ transitions. It has been emphasized recently[31] that the MO model does not correctly describe the weak metal–metal interaction in oligomeric d^8 systems; a valence-bond model is superior. However, the MO model does give a reasonable description of the lowest energy ($d\sigma^*$–$p\sigma$) excited states, and so is adopted here for the sake of simplicity. As suggested by their MO one-electron description, the ($d\sigma^*$–$p\sigma$) excited states show large excited-state distortions along the metal–metal coordinate corresponding to shorter metal–metal distances in the excited states; long vibronic progressions in the metal–metal vibrational frequency have been resolved in some cases.[22,30,31] The resulting low-temperature half-widths for the electronic absorption and emission bands are 1000–1500 cm^{-1}. Significant excited-state distortions in any ligand coordinate have not been detected for[23,30] $Pt_2(P_2O_5H_2)_4^{4-}$ or for valence-isoelectronic complexes of Rh(I) and Ir(I) with isocyanide ligands,[31] which suggests that the excitations are fairly pure $d \rightarrow p$ excitations for these materials.

We next consider a linear-chain case, the compound[32] $Pt(en)Cl_2$, which crystallizes in a linear-stack structure with a $d(Pt_2)$ of 3.381 Å. The $d_{z^2} \rightarrow p_z$ transition of the dilute monomer (z is taken to be perpendicular to the molecular plane) has been assigned[32] at 49 000 cm^{-1} (ϵ = 6600). The electronic spectrum of the crystal is very strongly perturbed from solution, which is attributable to the metal–metal interaction. While the levels of an "infinite" chain are properly described as bands,[12,14e] the group-theoretical treatment is very similar to the binuclear case. Thus, singlet and triplet "$d\sigma^* \rightarrow p\sigma$" excited states (top of the d_{z^2} band to bottom of the p_z band) are expected. According to a Hückel model, the stabilization of the lowest excited state for an infinite chain is just twice that for a binuclear complex with the same metal–metal separation. In actuality, the chain excited states are clearly rather localized[12] (precisely how localized is unclear at this time), so the linear-chain and binuclear cases may be still more similar than indicated by the Hückel model.

Crystalline $Pt(en)Cl_2$ exhibits[32] an intense absorption band at 285 nm (35 100 cm^{-1}) that is completely polarized parallel to the Pt-stacking direction (hereafter referred to as z). The ϵ is 55 100

(27) (a) Biedermann, J.; Wallfahrer, M.; Gliemann, G. *J. Lumin.* **1987**, *37*, 323. (b) Schwarz, R.; Lindner, M.; Gliemann, G. *Ber. Bunsen-Ges. Phys. Chem.* **1987**, *91*, 1233. (c) Biedermann, J.; Gliemann, G.; Klement, U.; Range, K.-J.; Zabel, M. *Inorg. Chem.* **1990**, *29*, 1884.

(28) We have checked the description[27a] of crystal properties (including absorption polarization) against the subsequently published crystal structure[5] of $Pt(bpy)(CN)_2$ and find that Gliemann et al. correctly assumed that the needle axis is the Pt-stacking axis. This axis has been labeled as the orthorhombic (*C2mm*) *c* axis in ref 5, rather than as the *a* axis in ref 27a.

(29) We have corrected these values from those estimated in ref 27a by using the X-ray-determined crystal density of ref 5.

(30) Rice, S. F.; Gray, H. B. *J. Am. Chem. Soc.* **1983**, *105*, 4571.

(31) Smith, D. C.; Miskowski, V. M.; Mason, W. R.; Gray, H. B. *J. Am. Chem. Soc.* **1990**, *112*, 3759 and references therein.

(32) Anex, B. G.; Peltier, W. P. *Inorg. Chem.* **1983**, *22*, 643.

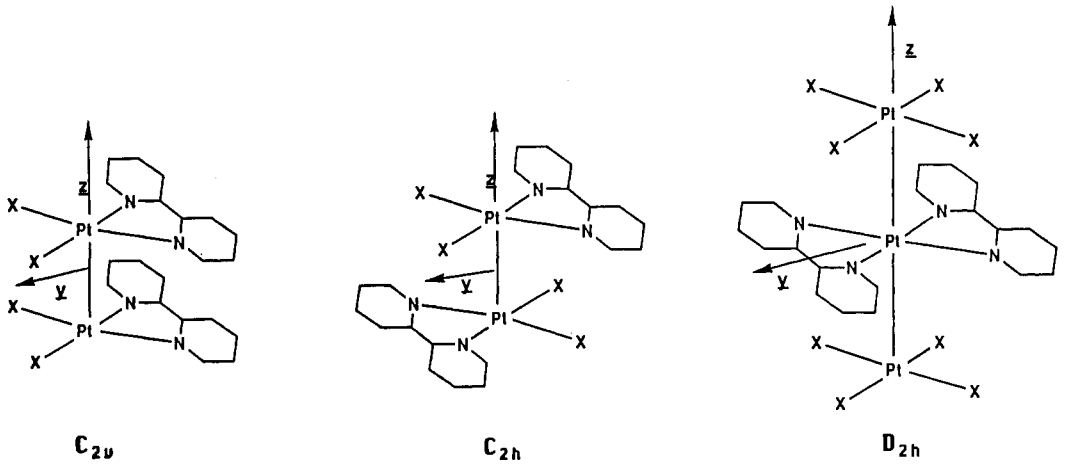

Figure 4. Structures for building blocks of Pt(II) α-diimine linear-chain compounds, with symmetry axes indicated. In each case, the minimum oligomer needed to express the chain symmetry is shown. In the C_{2v} case, the C_2 reflection axis is the y axis. In the C_{2h} case, the C_2 rotation axis is the x axis.

(equivalent to an isotropic ε of 55 100/3 = 18 400). This was assigned to the $^1(d\sigma^* \rightarrow p\sigma)$ transition, strongly red-shifted from the monomer $d_{z^2} \rightarrow p_z$ transition by the metal–metal interaction.

Martin[15a] has identified a second electronic transition that is not present for the solution chromophore, a sharp band at 302 nm (33 100 cm^{-1}) that is polarized perpendicular to z (ε = 600). While Martin proposed a "metal-to-metal charge-transfer" assignment, we suggest that assignment of this band to the $^3(d\sigma^* \rightarrow p\sigma)$ excitation is very reasonable. Martin did not consider spin-forbidden excitations in his analysis, but comparison to the binuclear systems discussed above indicates that they should have substantial intensity, and the energetic separation of 2000 cm^{-1} from the singlet–singlet transition is reasonable. Since several ligand-field excitations are located to lower energy of this band,[15a] emission from the d → p excited states should not be (and is not[33]) observed.

Next, consider the case of $Pt(CN)_4^{2-}$ salts, which commonly adopt a linear-stack structure. In contrast to the preceding example, where the Pt(II) d_{z^2} and p_z orbitals are considered to be fairly pure metal orbitals, the metal p_z orbital is considered[12] to mix with CN$^-$ π* orbitals in $Pt(CN)_4^{2-}$. An additional difference is that the strong-field CN$^-$ ligands push ligand field excited states to very high energy, so that d → (p, π*(CN)) states are the lowest energy excited states. The crystalline salts of $Pt(CN)_4^{2-}$ accordingly exhibit[12] both fluorescence (z-polarized, τ < 300 ps) and phosphorescence (x,y-polarized, τ in the microsecond to millisecond range). The compound $Ca[Pt(CN)_4]\cdot 5H_2O$ has a linear-chain structure with $d(Pt_2)$ = 3.38 Å, the same as for $Pt(en)Cl_2$. It exhibits[12] an intense z-polarized absorption at 24 400 cm^{-1} and a weak x,y-polarized absorption at 22 700 cm^{-1}. The ~10 000-cm^{-1} red shift of these features from the analogous transitions of crystalline $Pt(en)Cl_2$ presumably reflects the π*(CN) character of the (p_z, π*(CN)) LUMO of the "dσ* → pσ" transitions. Corresponding electronic emissions are observed at 22 250 cm^{-1} (fluorescence) and 20 700 cm^{-1} (phosphorescence).

We finally turn to the α-diimine complexes. Gliemann et al.[27a,b] assigned the emissions of $Pt(bpy)(CN)_2$ and $Pt(phen)(CN)_2$ to d → (p, π*(CN)) states that were presumed to be strictly similar to those of $Pt(CN)_4^{2-}$ linear-stack compounds. There are several reasons to doubt this assignment. By comparison to the linear-chain compound $Ba[Pt(CN)_4]\cdot 4H_2O$ ($d(Pt_2)$ = 3.321 Å and phosphorescence maximum at 513 nm (19 500 cm^{-1})), $Pt(bpy)(CN)_2$ has a nearly identical $d(Pt_2)$ (3.33 Å), yet emission is shifted 3000 cm^{-1} to lower energy. As noted earlier, the observation of vibronic structure in an α-diimine effective frequency unequivocally indicates α-diimine participation in the excited state. A fundamental reason to question the Gliemann assignment is that MLCT states involving α-diimine ligands typically lie at much lower energy than those for CN$^-$. A telling comparison[34] exists

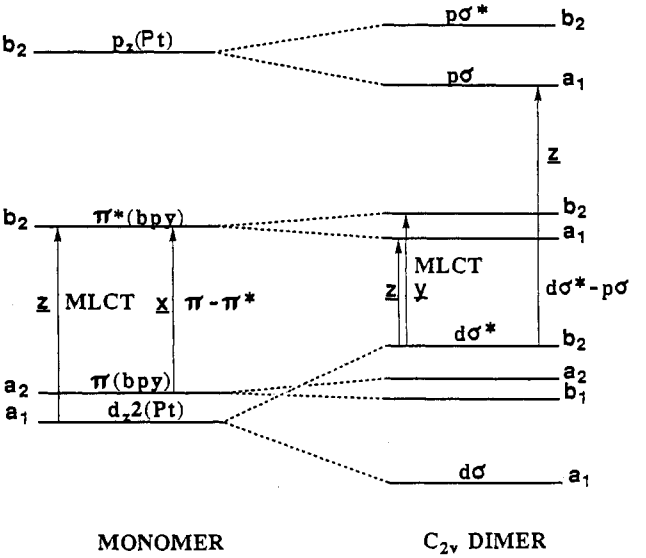

Figure 5. Proposed MO diagram for $Pt(bpy)X_2$ and its C_{2v}-symmetry oligomers.

between the Ru(II) complexes $Ru(bpy)_3^{2+}$ (lowest energy MLCT at 21 600 cm^{-1} (ε = 14 000)) and $Ru(CN)_6^{4-}$ (lowest energy MLCT at 48 800 cm^{-1} (ε = 37 000)). We therefore consider possible MLCT assignments involving the α-diimine ligands.

Figure 4 shows the minimum units that express the chain symmetry of the various types of α-diimine Pt(II) linear-chain compounds. The unit appropriate to $Pt(bpy)(CN)_2$, according to the crystal structure,[5] is the one designated C_{2v}, and Figure 5 shows its molecular orbital model. The molecular axes are chosen to maintain the z axis as the chain (perpendicular to the monomer plane) axis, with the y axis chosen to coincide with the bpy local C_2 rotation axis. In C_{2v} symmetry, we further choose the x and z axes to transform as B_1 and B_2, respectively. Gliemann et al.[27] chose different axes, and care is needed in comparing our treatments.

The monomer $Pt(bpy)(CN)_2$ has as its lowest IL π → π* transition the $a_2 \rightarrow b_2$ transition,[34] which is allowed with (in our axis convention) x-polarization, that is, "long-axis" bpy polarization. There is no doubt about the identification of the LUMO; the next highest energy π* levels of bpy are more than 6000 cm^{-1} to higher energy.[35] Among the monomer MLCT transitions, we consider only the $d_{z^2} \rightarrow \pi^*$, $a_1 \rightarrow b_2$ transition, which is allowed with z polarization. This is not necessarily the lowest energy monomer MLCT transition; the ordering of the filled monomer

(33) Houlding, V. H. Work in progress.
(34) Miskowski, V. M.; Gray, H. B. *Comments Inorg. Chem.* **1985**, *4*, 323.
(35) (a) Konig, E.; Kremer, S. *Chem. Phys. Lett.* **1970**, *5*, 87. (b) Kober, E. M.; Meyer, T. J. *Inorg. Chem.* **1984**, *23*, 3877. (c) Kober, E. M.; Meyer, T. J. *Inorg. Chem.* **1982**, *21*, 3967.

d orbitals in these compounds is unknown, although it can be anticipated[15a] that they will be closely spaced. However, the $d_{z^2} \rightarrow \pi^*$ MLCT will be uniquely and strongly perturbed by metal–metal interaction.[31] The right-hand side of Figure 5 shows the metal–metal perturbations that are expected. It can be seen that if the d_{z^2}(Pt) interaction is sufficiently strong to make a $d\sigma^*$ level the HOMO, the $d\sigma^* \rightarrow \pi^*$ MLCT transition may become lower in energy than the $\pi \rightarrow \pi^*$ IL transition. The MLCT transition yields two singlet–singlet transitions, corresponding to the two symmetry combinations of the π^* orbitals of the two bpy ligands. In the particular case of the C_{2v} dimer, these are of a_1 and b_2 symmetries and are bpy–bpy bonding and antibonding, respectively. While the $\pi \rightarrow \pi^*$ transitions of solid Pb(bpy)$(CN)_2$ do not appear to be strongly perturbed, even a weak interaction should establish the energetic ordering $b_2 > a_1$; moreover, the interaction may be stronger in the excited state[2] (excimeric). The lowest energy MLCT transition should therefore be $b_2(d\sigma^*) \rightarrow a_1(\pi^*$(bpy)), $^1A_1 \rightarrow {}^1B_2$, which is dipole-allowed with z-polarization. The corresponding $^3B_2$ state has spin–orbit components of A_1, B_1, and A_2 symmetries, the first two yielding dipole-allowed transitions with the ground state of respectively y- and x-polarization, that is, perpendicular to z.

These predictions are all in accord with experiment. Note, moreover, that since these transitions transform identically with the $b_2 \rightarrow a_1$ singlet and triplet $d\sigma^* \rightarrow (p\sigma, \pi^*(CN))$ transitions, *all* of the extensive single-crystal experiments performed by Gliemann's group[27] that were shown to be consistent with the d→p assignment are actually equally consistent with our assignment.

Consideration of MO schemes similar to Figure 5 for C_{2h} and D_{2h} stacking patterns (Figure 4) yields similar predictions; $d\sigma^* \rightarrow \pi^*$(bpy) MLCT is always predicted to be dipole-allowed parallel to z for the singlet–singlet transition and perpendicular to z for the singlet–triplet transition. There are two complications, however. First, the dipole-allowed MLCT transitions are always accompanied by Laporte-forbidden ones (since there are two combinations of the bpy π^* orbitals; a_g and b_u for the C_{2h} unit, b_{3g} and b_{1u} for the D_{2h} unit), and there is, in contrast to the case of the C_{2v} unit, no obvious way to predict their energetic ordering. Thus, gerade-symmetry MLCT states could conceivably end up as the lowest energy ones, which would result in a more complicated (vibronically allowed) emission behavior. A second complication is that, for the C_{2h} stacking pattern, molecular z-polarization can in principle be mixed with y-polarization. However, the absorption data for Pt(en)Cl_2 show[33] no such effect.

We note that in a very recent paper[36] Gliemann et al. have adopted an assignment scheme somewhat similar to our present one. The similarity is a rather formal one, since they label their LUMO as (using our notation) a (p_z(Pt), π^*(CN), π^*(α-diimine)) orbital, thus begging the question of the best description of the electronic transition (and continuing to deemphasize the α-diimine contribution). Mixing among all these orbitals is, of course, symmetry-allowed and undoubtedly occurs to some extent. However, since the IL transitions of the α-diimine ligands are not greatly perturbed, we feel that it is reasonable to simply write the LUMO as a π^*(α-diimine) orbital for the compounds of this study.

We finally consider the interesting variation in the Huang–Rhys ratio S for the α-diimine effective vibration among the various compounds of this study (compare Figures 1 and 3). One possible explanation we considered was that the C_{2v} stack structure of Pt(bpy)$(CN)_2$ might affect S via bpy–bpy interactions. However, we have recently[33] determined emission spectra at 10 K for the compound Pt(bpy)Cl_2, which has the C_{2h} stack structure with[4] $d(Pt_2)$ = 3.40 Å at room temperature. The spectral profile (maximum at 15 400 cm^{-1}) is nearly identical with that of Pt(bpy)$(CN)_2$, with S for the ~1400-cm^{-1} effective frequency being very similar. It may be noted that very large variations in S for the MLCT emissions of various Os(II) and Ru(II) bpy complexes have also been noted,[19b] and an explanation has been offered in terms of variations in the amount of mixing of the ligand π-symmetry levels with metal d orbitals as a function of charge and other ligands; a similar explanation may apply here.

Conclusions

The lowest energy excited states of isolated Pt(II) complexes of the α-diimine ligands of this study are diimine ^{3}IL states (except when weak-field ligands also in the complex drop a ligand field state below the ^{3}IL state),[2] but α-diimine MLCT states lie not far to higher energy. In this connection, we note that ligands that are substantially better electron acceptors than the simple α-diimines of this study could conceivably make a ^{3}MLCT state the lowest energy excited state, so these results are not necessarily generalizable. In particular, Pt(II) complexes of orthometalated aromatics[7] are not directly comparable, as these unusual ligands contribute their own complicated electronic structure to the picture and are not easily ranked among the more usual acidoamine and α-dimine ligands in terms of, e.g., electron-donating and/or -accepting ability.

Metal–metal interaction in polynuclear linear-chain Pt(II) compounds can greatly increase the energy of the $d\sigma^*$ combinations of metal d_{z^2} orbitals, which should clearly lower the energy of $d\sigma^* \rightarrow \pi^*$ MLCT relative to monomer $d_{z^2} \rightarrow \pi^*$ MLCT. We contend that this effect causes this type of MLCT state to be the lowest energy excited state in the linear-chain compounds of this study. For Pt–Pt distances that are longer than the 3.3–3.4 Å of our compounds, the ^{3}IL state should eventually become the lowest energy excited state even for dimeric or linear-chain structures; this was our proposal[2] for the emission of the compound $[Pt(phen)_2]Cl_2 \cdot 3H_2O$, and another example has been recently presented[27c] for the compound Pt(bipyrimidine)$(CN)_2$.

A final interesting question is whether very short Pt–Pt distances might make a d → p or d → (p, π^*(CN)) state the lowest energy excited state for an α-diimine complex. The phosphorescence of $Pt(CN)_4^{2-}$ salts becomes roughly isoenergetic with that observed for Pt(bpy)$(CN)_2$ when $d(Pt_2)$ becomes about 3.15 Å.[12] It must be remembered, however, that the MLCT states would also be strongly red-shifted for such a short $d(Pt_2)$, and ^{3}MLCT would probably still be the lowest energy excited state.

Acknowledgment. We thank C.-M. Che, C. Frito, and G. Gliemann for helpful comments and C.-M.C. in particular, for initially provoking our research on neutral-stack compounds by donating several samples. We are also grateful to Dr. Jordi Marti (Allied-Signal Inc.) for his work on the X-ray and TEM results. A preliminary version of this work was presented at the 8th ISPPCC, Santa Barbara, CA, August 1989.

Registry No. $Na_2Pt(CN)_4$, 15321-27-4; $[Pt(bpy)(en)](ClO_4)_2$, 54806-37-0; [Pt(bpy)(en)][Pt$(CN)_4$], 136503-94-1; [Pt(phen)(en)][Pt$(CN)_4$], 136503-95-2; $[Pt(bpy)_2][Pt(CN)_4] \cdot 2H_2O$, 136503-96-3; $[Pt(bpy)_2][Pt(CN)_4]$, 54806-40-5; $[Pt(phen)_2][Pt(CN)_4]$, 59981-69-0; Pt$(bpy)(CN)_2 \cdot xH_2O$, 136503-97-4; Pt(bpy)$(CN)_2$, 54806-39-2; Pt(phen)$(CN)_2$, 54806-38-1.

(36) Biedermann, J.; Gliemann, G.; Klement, U.; Range, K.-J.; Zabel, M. *Inorg. Chim. Acta* **1990**, *169*, 63.